

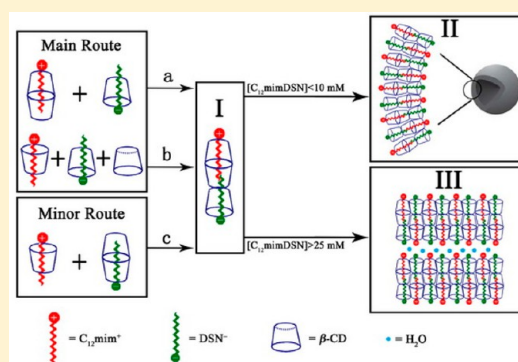
Construction of Supramolecular Self-Assemblies Based on the Biamphiphilic Ionic Liquid– β -Cyclodextrin System

Jianfeng Shi and Xinghai Shen*

Beijing National Laboratory for Molecular Sciences (BNLMS), Fundamental Science on Radiochemistry and Radiation Chemistry Laboratory, College of Chemistry and Molecular Engineering, Peking University, Beijing 100871, P. R. China

Supporting Information

ABSTRACT: A new kind of biamphiphilic ionic liquid (BAIL) consisting of 1-dodecyl-3-methylimidazolium ($C_{12}mim^+$) and dodecyl sulfonate (DSN^-) has been synthesized and characterized for the investigation on its self-assembling behavior with β -CD in the aqueous medium. Vesicles were found in the diluted $C_{12}mimDSN@3\beta$ -CD solution, and on increasing the concentrations of both IL and β -CD, the solution turned into a white hydrogel, which showed a temperature-dependent sol–gel transition. The building block consisting of one $C_{12}mimDSN$ and three β -CDs was proposed, and a novel self-assembly mechanism was studied. Both cation and anion of the BAIL are involved in the self-assembling with β -CD. The electronic interaction between $C_{12}mim^+$ and DSN^- , the hydrophobic interaction between the alkyl chains of BAIL and β -CD cavity, H-bond between neighboring β -CDs, and the interaction between imidazolium headgroup and water in the hydrogel are the driving force for the self-assembly.



INTRODUCTION

Cyclodextrins (CDs) are a series of doughnut-like macrocyclic oligosaccharides which can encapsulate various molecules in their cavities to form inclusion complexes by the hydrophobic interaction and/or H-bonding.^{1–5} CDs are commercially available, nontoxic, and water-soluble, making them widely used in the pharmaceutical industry, foodstuffs, daily use, chemical industry, etc.^{6,7} As a result of their unique structures and properties, CDs can be closely related to many interesting topics such as molecular recognition, self-assembly, and inclusions for different functional components. The CD inclusion complex is one of the most important structures in the field of ordered supramolecular self-assembly chemistry. Aggregates such as micelles,⁸ vesicles,^{9–15} microtubes,^{16,17} and the supramolecular hydrogel^{11,18–21} can be constructed based on the inclusion complexation between CD and various kinds of guest molecules.

Ionic liquids (ILs) have attracted increasing attention in recent years due to their desirable properties such as easy recyclability, nonflammability, high ionic conductivity, wide electrochemical potential window, low vapor pressure, and high thermal stability. They have been regarded as promising solvents in organic syntheses, catalyzes, separations, solar cells, and so on.^{22–25} The investigation on the interaction mechanism between an IL and β -CD is of great importance, and there have already been some reports on this subject.^{26–30} Among various kinds of ILs, surface-active ILs, which possess long alkyl chain and exhibit surface active property in their aqueous solutions, are particularly interesting. In the earlier reports, several surface-active ILs were synthesized and their

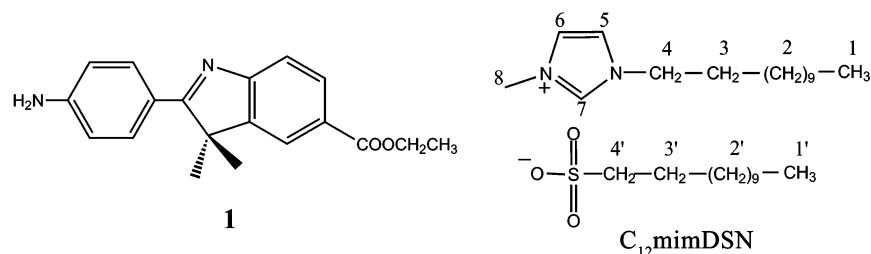
aggregation behaviors were investigated.^{31–35} It was found that the long chain imidazolium ILs show superior surface activity and versatility in functionalization as compared with the traditional ionic surfactants. Moreover, the surface-active ILs can also form stable inclusion complexes with CDs.^{26–28} However, to our knowledge, there are few reports on the self-assembling behavior of CDs with surface-active ILs.

Our research group has been investigating the supramolecular behavior between imidazolium-based ILs and β -CD in the past several years.^{36–40} In the diluted aqueous solution, it was found that the imidazolium-based ILs and β -CD can form 1:1 (guest:host), 1:2 inclusion complexes, or both.^{36–39} Very recently, we have found the formation of vesicle in the concentrated aqueous solution of 1-dodecyl-3-methylimidazolium bromide ($C_{12}mimBr$) and β -CD, which can transform into a novel supramolecular hydrogel upon the decrease of temperature.⁴⁰ With an increase in the concentration of $C_{12}mimBr@\beta$ -CD system, the transition temperature is also increased. According to the XRD and the 1H – 1H ROESY NMR spectrum, the simple inclusion complex between $C_{12}mim^+$ and β -CD constructs the basic block of the lamellae, with the two alkyl side chains of the $C_{12}mim^+$ intersecting with each other in the β -CD cavity. The H-bonding between β -CDs, β -CD and water, and the imidazolium headgroup of $C_{12}mim^+$ and water contribute to the formation of the vesicle and the supramolecular hydrogel.⁴⁰

Received: November 18, 2013

Revised: January 4, 2014

Published: January 22, 2014

Scheme 1. Structures of the Fluorescence Probe **1** and C_{12} mimDSN

However, in the C_{12} mimBr@ β -CD self-assembly system, the role of the anion Br^- in the formation of the supramolecular structure is not clear yet. As an inorganic anion, Br^- may just help keep the electrical neutrality. By changing the anion of IL, we discovered that the C_{12} mimCl@ β -CD solution can also form vesicle and supramolecular hydrogel.⁴⁰ And preliminary experiments revealed that no hydrogel exists in the concentrated C_{12} mimBF₄@ β -CD solution. The reason may be that the anion BF_4^- with hydrophobic characteristic can also interact with β -CD,³⁷ thus disturbing the formation of the vesicle and the hydrogel. In this article, a new kind of biamphiphilic ionic liquid (BAIL)⁴¹ is synthesized to design the supramolecular assemblies with β -CD. The role of the anion in the self-assembling behavior can be examined. The BAIL is a special kind of salt-free catanionic surfactant with amphiphilic characteristic in both the constituent ions. They are supposed to behave as catanionic surfactants with improved surface activity and capability of forming a variety of self-assembled structures.⁴¹

The chemical properties of a common catanionic surfactant have been well characterized in recent years. The most obvious feature is that they can spontaneously self-assemble into various kinds of microstructures in aqueous solution.^{42–49} In the field of CD supramolecular chemistry, the interaction and aggregation behavior between CD and catanionic surfactant were also reported.^{50–53} Yan et al.^{50,51} suggested that β -CD forms inclusion complexes with both cationic and anionic parts of the catanionic surfactant without significant selectivity. Besides, the inclusion of β -CD with catanionic surfactants can destroy the ion pair and the aggregates of catanionic surfactants and even inhibit their precipitation. But no further studies were performed on the supramolecular self-assembling behavior between catanionic surfactant and β -CD. Jiang et al.⁵² investigated the inclusion phenomenon of β -CD in the nonstoichiometric mixed cationic and anionic surfactant system. The selective binding of β -CD with the excess component of the surfactants shifts the surfactant composition to an electroneutral stoichiometry and thus gives rise to a micellar elongation and a micelle-to-vesicle transition. A similar mechanism for the aggregation transition was also proposed by Wang et al.⁵³ However, in these examples, the self-assemblies were merely constitutive of the catanionic surfactants. β -CD did not participate in self-assembling as a structural unit but only formed inclusion complexes with the free ionic surfactant.

So far, there has been no report about that catanionic surfactants or BAILs form self-assemblies with β -CD. It has been discovered that β -CD forms inclusion complexes with both cationic and anionic parts of the catanionic surfactant, and the inclusion of β -CD with catanionic surfactants can dismantle the ion pair and thus destroy the aggregates of catanionic surfactants.⁵¹ Besides, β -CD can self-assemble with either a cationic-type IL or an anionic-type surfactant in the aqueous

medium.^{13,16,40} So we believe that the self-assemblies consisting of BAILs and β -CD should exist.

EXPERIMENTAL SECTION

Materials. C_6 mimBr, C_8 mimBr, C_{10} mimBr, and C_{12} mimBr (>99%) were purchased from Lanzhou Institute of Chemical Physics (China). The synthesis and purification of the fluorescent probe 2-(*p*-aminophenyl)-3,3-dimethyl-5-carboxyethylindole (**1**, shown in Scheme 1) were done according to the literature.^{54,55} Cetyltrimethylammonium bromide (CTAB, 98%, Sigma-Aldrich), sodium dodecyl sulfonate (SDSN, $\geq 98.5\%$, Beijing Chemical Reagents Co.), α -CD ($\geq 98\%$, ACROS), γ -CD ($\geq 99\%$, ACROS), 2,6-dimethyl- β -CD (DM- β -CD, J&K Chemical Co.), hydroxypropyl- β -CD (HP- β -CD, J&K Chemical Co.), NaBr (AR, Beijing Chemical Works), NaCl (AR, Beijing Chemical Works), $MgCl_2$ (AR, Beijing Yili Fine Chemical Co.), and $Al(NO_3)_3$ (AR, Beijing Yili Fine Chemical Co.) were used as received. β -CD ($\geq 98\%$, Beijing Aoboxing Biotech Co.) was recrystallized twice using tridistilled water and dried under vacuum at 110 °C for 24 h. D_2O (99.9% isotopic purity, Beijing Chemical Reagents Co.) was used as solvent in NMR measurements. Tridistilled water was used throughout the experiments.

C_{12} mimDSN (Scheme 1), a new kind of BAIL, was synthesized via an anion exchange reaction according to the literature.⁴¹ An equimolar mixture of C_{12} mimBr and SDSN was dissolved in water and stirred at 60 °C for 3 h. Water was removed from the reaction mixture using a rotary evaporator, and the mixture was extracted with dichloromethane to filter off NaBr. After that the organic phase was washed several times with water until the complete removal of Br^- (monitored with 0.1 M $AgNO_3$) and then completely dried prior to use. The corresponding ¹H NMR result is ¹H NMR (400 MHz, TMS- CH_2Cl_2), δ H (ppm) 0.880 (t, 6H; two CH_3), 1.250 (m, 36H; two alkyl chains), 1.854 (p, 2H; CH_2), 2.044 (p, 2H; CH_2), 2.860 (t, 2H; CH_2), 4.065 (s, 3H; CH_3), 4.265 (t, 2H; CH_2), 7.254 (d, 2H; two CH), 10.108 (s, H; CH). And the elementary analysis result (sample: 5.57% H, 67.21% C, and 11.09% N; theoretical value: 5.59% H, 67.15% C, and 11.27% N) also confirmed the high purity of the obtained C_{12} mimDSN. C_{10} mimDSN, C_8 mimDSN, C_6 mimDSN, and CTA-DSN were also synthesized by the same method.

Methods. Sample Preparation. The C_{12} mimDSN and β -CD solutions were prepared by weighing a desired amount of C_{12} mimDSN and β -CD into tubes and then heating to obtain transparent solutions, which were then kept thermostatically at room temperature for at least 24 h. Depending on the concentrations of the samples, transparent solutions, precipitate, or white hydrogel could be obtained. The xerogel was obtained by freeze-drying for about 36 h after the hydrogel was quickly frozen by liquid nitrogen.

UV-vis Analysis. The UV-vis analysis was recorded on a Hitachi 3010 UV-vis spectrometer. The sample was placed in a 1 cm path length quartz cell. In the sol-gel transition observation, the temperature was controlled by placing the sample in the quartz cell in a compartment whose walls were accessible to water circulation. The samples were kept for at least 10 min to reach equilibrium, and the final temperature was obtained by a thermocouple (Check-temp, Hanna, Italy).

Dynamic Light Scattering (DLS). DLS measurements were performed on an ALV/DLS/SLS-5022F photocalorimeter spectrometer. The wavelength of laser was 632.8 nm, and the scattering angle was 90°. The temperature was controlled at 25 °C. The samples were treated by centrifugating at 12 000 rpm for 30 min before the measurement.

Transmission Electron Microscope (TEM). The negative-staining TEM samples were examined on an FEI Tecnai G2 T20 electron microscope operating at 200 kV. One drop of the sample solution was placed onto a Formvar-coated copper grid, and a drop of phosphotungstic acid solution (2 wt %) was used as the staining agent to make the TEM images more clear. For the freeze-fracture transmission electron microscopy (FF-TEM), samples were frozen by liquid propane. The fracturing and replication were carried out on a freeze-fracture apparatus (Balzers BAF400, Germany) at -140 °C. Pt/C was deposited at an angle of 45° to shadow the replicas, and C was deposited at an angle of 90° to consolidate the replicas. The resulting replicas were also examined on an FEI Tecnai G2 T20 electron microscope operating at 200 kV.

Differential Scanning Calorimeter (DSC). DSC measurements were performed on a Q100 instrument upon heating or cooling the samples at the rate of 4 °C/min.

Fourier Transform Infrared Spectra (FTIR). FTIR spectra of the grinded xerogel were recorded on a NICOLET iN10 MX spectrometer using the infrared microspectroscopy method.

Scanning Electron Microscope (SEM). SEM of the grinded xerogel was conducted on FEI Nova NanoSEM 430 at 1 kV.

Powder X-ray Power Diffraction (XRD). XRD patterns were obtained on a D/MAX-PC2500 diffractometer with Cu K α radiation ($\lambda = 0.154\ 056\ \text{nm}$). The supplied voltage and current were set to 40 kV and 100 mA, respectively. Powder samples were mounted on a sample holder and scanned from 3° to 30° of 2θ at a speed of 4°/min.

High-Resolution Mass Spectrometry (HRMS). The HRMS used with electrospray ionization (ESI) was done on a Fourier transform ion cyclotron resonance mass spectrometer, APEX IV (Bruker).

Competitive Fluorescence Method. Substituted 3H-indoles have been used as fluorescence probes to study CD-based supramolecular systems in our previous studies.^{36–39,56} Here a stock solution of **1** was prepared in methanol, and 50 μL aliquots of this stock solution were added into 5 mL volumetric flasks to maintain a final concentration of $10^{-6}\ \text{M}$ for fluorescence measurements. The pH value of all the solutions in this study was adjusted to 9.5 by adding NaOH, and no buffer was used.⁵⁶ At low fluorescence probe concentrations, the total fluorescence intensity of **1** in **1**/ β -CD solutions can be expressed by eq 1 with different initial concentrations of β -CD ($[\text{CD}]_0$), which ranged from 0 to 4.4 mM.

$$I = \frac{(I_0 + I_1K'_1[\text{CD}]_0 + I_2K'_1K'_2[\text{CD}]_0^2)}{1 + K'_1[\text{CD}]_0 + K'_1K'_2[\text{CD}]_0^2} \quad (1)$$

The K'_1 , K'_2 , I_1/I_0 , and I_2/I_0 values (K'_1 and K'_2 are the association constants for 1:1 and 1:2 complexes between **1** and β -CD, and I_0 , I_1 , and I_2 stand for the fluorescence intensity of **1** in pure water, in the 1:1 complex, and in the 1:2 complex, respectively) can be estimated by nonlinear regression analysis. The equilibrium concentration of β -CD, i.e., $[\text{CD}]$, at different $[\text{SDSN}]_0$ (the initial concentration of SDSN) can be calculated using the K'_1 , K'_2 , I_1/I_0 , and I_2/I_0 values according to eq 1. After that, the fluorescence spectra of **1** in the SDSN- β -CD system were measured. The $[\text{SDSN}]_0$ ranged from 0 to 5.5 mM, whereas the $[\text{CD}]_0$ was fixed to 4 mM. According to the literature, the fluorescence intensity of **1** at 4 mM of β -CD reaches a plateau, showing that most molecules of **1** exist in 1:2 complexes, and thus the 1:1:1 (guest A:guest B:host) ternary complex between **1**, DSN⁻, and β -CD can be assumed not to form.⁵⁶ Thus, by analyzing the variation of $[\text{SDSN}]_0$ as a function of $[\text{CD}]$ with eq 2 for 1:1 and 1:2 inclusion complexation, the results of the interaction between β -CD and SDSN can be obtained.^{38,39} All the fluorescence spectra were measured on an FL-4500 (Hitachi, Japan) spectrofluorometer.

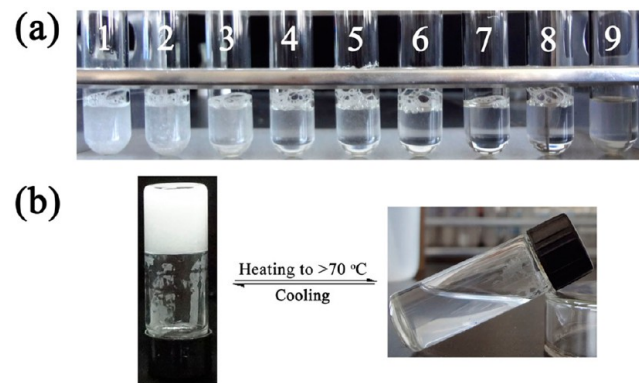
$$[\text{SDSN}]_0 = \frac{([\text{CD}]_0 - [\text{CD}])(1 + K_1[\text{CD}] + K_1K_2[\text{CD}]^2)}{K_1[\text{CD}] + 2K_1K_2[\text{CD}]^2} \quad (2)$$

Nuclear Magnetic Resonance (NMR). The spectrum of ^1H - ^1H ROESY NMR was recorded on Bruker AV400 MHz NMR spectrometer with a mixing time of 300 ms in the phase-sensitive mode.

RESULTS AND DISCUSSION

Macroscopic Phenomena of C₁₂mimDSN and β -CD Solutions. It is well-known that most of the equimolar mixtures of cationic and anionic surfactants form precipitate or become turbid at very low concentration.^{57,58} In our experiment, the appearance of 4 mM C₁₂mimDSN solution was turbid at room temperature, and the solid precipitate would generate when it was kept on standing (sample 1 in Scheme 2a). However, the amount of the precipitate decreased, and the

Scheme 2. (a) Photographs of the C₁₂mimDSN and β -CD Solution at Room Temperature;^a (b) Sol-Gel Transition of the C₁₂mimDSN@ β -CD (30 mM@90 mM) Hydrogel



^aThe concentration of C₁₂mimDSN is 4 mM, and the concentration of β -CD is (1) 0, (2) 4, (3) 8, (4) 10, (5) 10.5, (6) 11, (7) 11.5, (8) 12, and (9) 16 mM.

solution gradually turned transparent by adding β -CD (Scheme 2a). When the molar ratio of β -CD to C_{12} mimDSN reached 3, a transparent solution was obtained (sample 8 in Scheme 2a). This process was monitored by the UV absorbance of the solution at 650 nm in UV-vis spectroscopy, as there is no absorbance at 650 nm for the aqueous solution of either C_{12} mimDSN or β -CD. As is shown in Figure 1, a dramatic

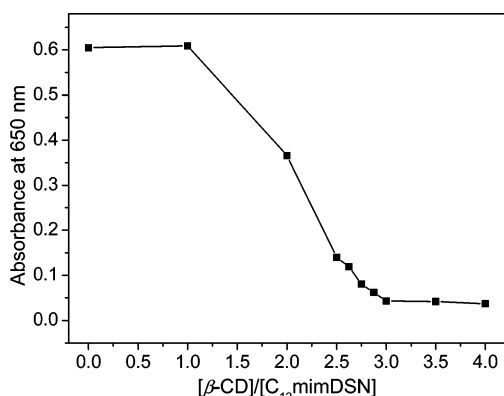


Figure 1. UV absorbance at 650 nm of the solutions with 4 mM C_{12} mimDSN and different concentrations of β -CD.

decrease in the absorbance is observed with an increase in the molar ratio of β -CD to C_{12} mimDSN, indicating that the solution turns clear. The absorbance reaches a minimum at the molar ratio of β -CD to C_{12} mimDSN of 3, indicating that the 1:3 stoichiometry is necessary. The supramolecular self-assemblies found in the C_{12} mimDSN@ 3β -CD solution will be characterized below.

At room temperature, the maximum concentration of C_{12} mimDSN in the C_{12} mimDSN- 3β -CD solution was found to be about 10 mM, above which precipitation would take place. However, when the concentration of C_{12} mimDSN@ 3β -CD further increased to 30 mM@90 mM, a white uniform hydrogel was obtained. The C_{12} mimDSN@ 3β -CD solution at low concentration could not gelate when cooled to 4 °C, indicating that a relative high concentration of the C_{12} mimDSN@ 3β -CD system is necessary for gelation.

Compared with the C_{12} mimBr@ β -CD supramolecular hydrogel system,⁴⁰ the C_{12} mimDSN@ 3β -CD system exhibits a lower minimum concentration (25 mM@75 mM) to form the hydrogel and a higher sol-gel transition temperature. We may conclude that both the cation C_{12} mim⁺ and the anion DSN⁻ in C_{12} mimDSN should be involved in a more complex supramolecular structure.

Characterization of Vesicle. Typical C_{12} mimDSN@ 3β -CD transparent solution shows an obvious Tyndall phenomenon, suggesting the formation of microaggregates. The DLS measurement has been well established to characterize particles in the range of 1–1000 nm. Figure 2a shows the DLS result of the C_{12} mimDSN@ 3β -CD (4 mM@12 mM) solution. We can observe a peak at about 51 nm, and the hydrodynamic radius distribution ranges from 30 to 200 nm, indicating the existence of self-assemblies in different sizes.

TEM methods including negative-staining, FF-TEM, cryo-TEM, etc., have been widely applied in observing supramolecular self-assemblies such as vesicles and microtubes.^{8–16,40} The sizes and the morphologies of the self-assemblies in the C_{12} mimDSN@ 3β -CD solutions are examined by negative-staining TEM and FF-TEM. In Figure 3A,B,

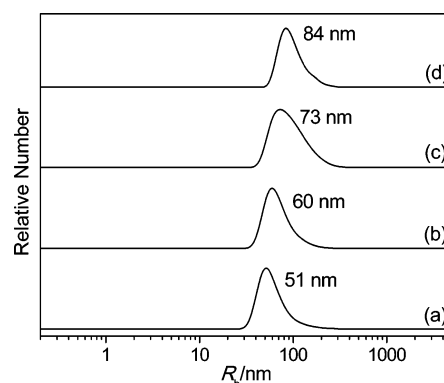


Figure 2. DLS results of the aqueous solutions of 4 mM C_{12} mimDSN and β -CD at (a) 12, (b) 14, (c) 16, and (d) 18 mM.

spherical particles with diameters ranging from 30 to 200 nm are readily verified. The shapes of some big size particles are irregular, indicating that they are probably rupture vesicles which burst when they are dried on the copper grids. In Figure 3C,D of FF-TEM, particles with diameters ranging from 80 to 350 nm are observed. Their shape also corresponds to vesicles after being fractured and replicated. Therefore, the TEM characterizations demonstrate the formation of spherical vesicles in C_{12} mimDSN@ 3β -CD solution.

The difference of vesicle sizes obtained by the two TEM methods should be understandable when taking the sample preparation methods into consideration. The vesicles in negative-staining TEM undergo a drying procedure, which may shrink the vesicles and even cause bursting. However, the FF-TEM samples are rapidly frozen by liquid propane; thus, the shape and size can be kept to a great extent. Moreover, the TEM method measures the solid spheres, while the DLS method measures the hydrodynamic radius of the swollen spheres. Besides, DLS gives the statistical result of the size distributions, while TEM reflects the local result of the assemblies in the solution.⁴⁰ Thus, the difference in the size distribution by DLS and FF-TEM is reasonable.

Characterization of Supramolecular Hydrogel. At a relatively high concentration, the C_{12} mimDSN@ 3β -CD solution turns into a white hydrogel at room temperature. As is shown in Figure 4A, the sol-to-gel and gel-to-sol transitions are monitored by the absorbance at 650 nm in UV-vis spectroscopy. The hydrogel turns into a turbid emulsion when the temperature increases to about 30 °C. With a further increase of the temperature to >70 °C, it finally becomes a transparent solution. With the decrease of the temperature, the reversibility of the transition is observed. The sol-gel transition temperature (T_{gel}) and the heat effect of the phase transition (ΔH) between sol and hydrogel were monitored by DSC measurement. In Figure 4B, a sharp endothermic peak in the heating curve and a broad exothermic peak in the cooling curve can be observed. The dotted line shows that the T_{gel} values in both the heating and cooling procedures are approximately the same (30.2 °C), which coincides with the transition temperature from the UV-vis method. After analyzing the results with the software Universal Analysis 2000, we can know that the ΔH values in the heating and the cooling procedures are 0.37 ± 0.04 and -0.54 ± 0.07 J/g, respectively, corresponding to about 12 ± 1 and 18 ± 2 kJ/mol of the C_{12} mimDSN@ 3β -CD unit. Moreover, several heating-cooling cycles have been performed

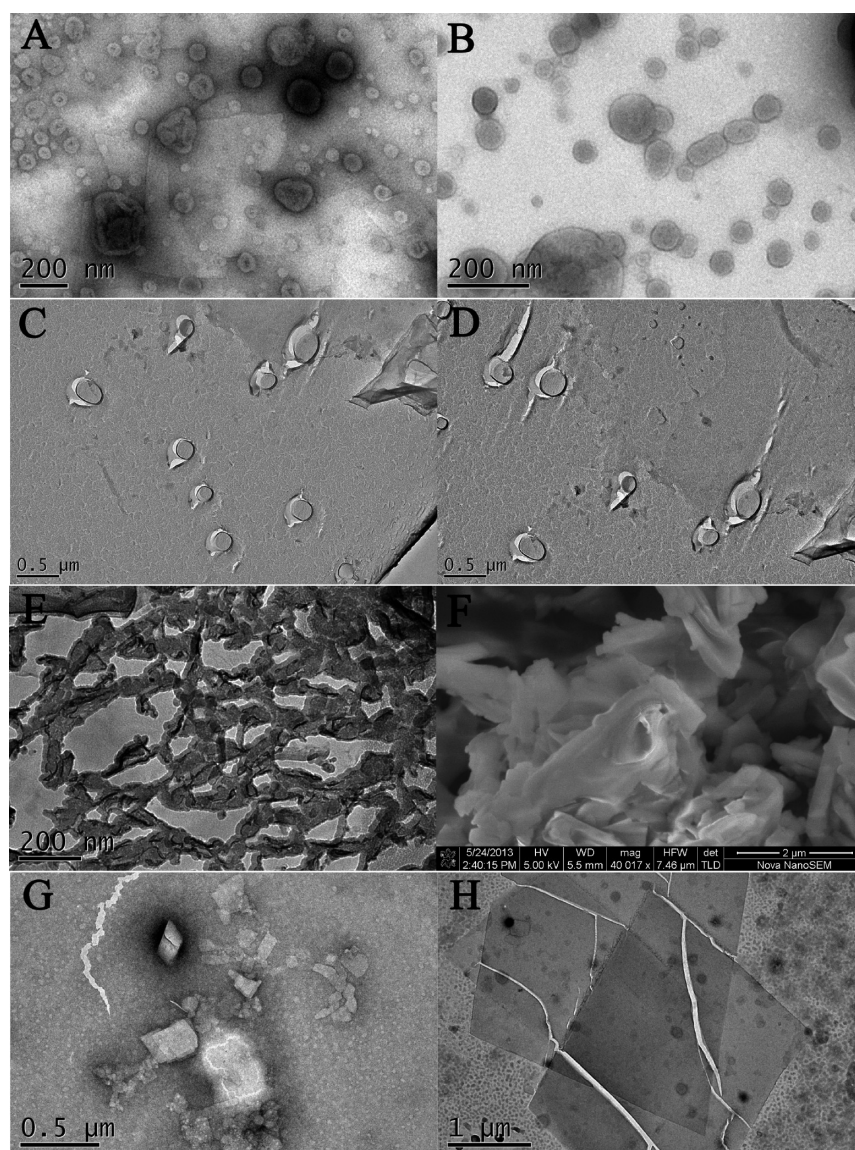


Figure 3. (A, B) Negative-staining TEM and (C, D) FF-TEM micrographs of the $C_{12}mimDSN@3\beta-CD$ (4 mM@12 mM) solution. (E) FF-TEM image of the $C_{12}mimDSN@\beta-CD$ (30 mM@90 mM) hydrogel and (F) SEM image of the corresponding xerogel. (G) The $\beta-CD$ aggregates in the 4 mM $C_{12}mimDSN$ and 18 mM $\beta-CD$ solution. (H) Negative-staining TEM of the $C_{12}mimDSN@3\beta-CD$ (15 mM@45 mM) solution.

on the same sample, confirming the reversibility of the sol–gel transition.

The structure of the hydrogel was studied by various methods. The FF-TEM image of the supramolecular hydrogel in Figure 3E shows a complex network phase. In order to obtain more information about the hydrogel, one can freeze-dry the sample and grind them to get the xerogel. By the SEM method, the xerogel shows a lamellar structure in Figure 3F.

TGA measurement reveals that the xerogel, after being freeze-dried for 36 h, still keeps water of about 9 wt %. The molar ratio of H_2O to the $C_{12}mimDSN@3\beta-CD$ unit in the xerogel is about 21, which indicates that the xerogel maintains the H-bonding network of the hydrogel and the characterization of the xerogel helps understand the structure of the hydrogel. In the FTIR measurement, we used D_2O instead of H_2O to prepare the hydrogel and then obtained the D_2O -xerogel. The D_2O shows its O–D stretching vibration peak at about 2500 cm^{-1} ,⁵⁹ so it does not overlap with the O–H stretching vibration peak of $\beta-CD$. The spectrum of the D_2O -

xerogel in Figure 5b is quite similar to that of $\beta-CD$, suggesting that the framework of xerogel mainly consists of $\beta-CD$ molecules. $C_{12}mimDSN$ only exhibits its characteristic absorption peak at 2854 cm^{-1} in the xerogel, suggesting that it is included in the $\beta-CD$ cavity in the structure. The spectrum of $\beta-CD$ shows the symmetric and antisymmetric O–H stretching vibration peak at 3375 cm^{-1} ,⁶⁰ while in xerogel, it shifts to a lower frequency at 3361 cm^{-1} . This evident change of the wavenumber clearly reflects the association of O–H groups which makes the stretching peak shift to a lower frequency.^{40,61} Therefore, we can conclude that the intermolecular H-bonding between neighboring $\beta-CD$ s as well as between $\beta-CD$ and water should contribute a lot to the formation of the supramolecular hydrogel.

The XRD patterns of $C_{12}mimDSN$, xerogel, $\beta-CD$, and the physical mixture of $C_{12}mimDSN@3\beta-CD$ are all listed in Figure 6 for comparison. The pattern (d) of the physical mixture is apparently the combination of the patterns of $C_{12}mimDSN$ and $\beta-CD$, while the pattern (b) of the xerogel is

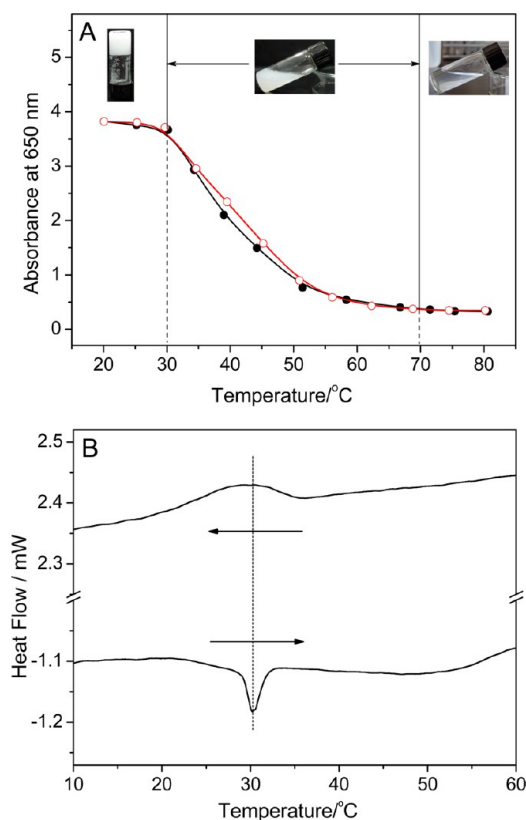


Figure 4. (A) Sol-to-gel (●) and gel-to-sol (○) transitions of the $C_{12}mimDSN@3\beta-CD$ (30 mM@90 mM) hydrogel monitored by the absorbance at 650 nm. (B) DSC heating and cooling curves of the $C_{12}mimDSN@3\beta-CD$ (30 mM@90 mM) hydrogel.

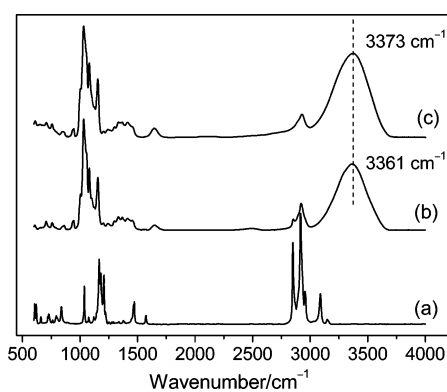


Figure 5. FTIR absorption spectra of (a) $C_{12}mimDSN$, (b) D_2O -xerogel, and (c) $\beta-CD$.

not. This reveals that the $C_{12}mimDSN$ and $\beta-CD$ molecules in both the xerogel and the hydrogel are regularly reorganized, which will be discussed below.

Mechanism of the Formation of Supramolecular Structures. Before the discussion of the self-assembly mechanism, it is necessary to confirm the participation of $\beta-CD$ in the self-assembly. The addition of $\beta-CD$ is usually believed to weaken or even destroy surfactant aggregates or surface-active molecule aggregates. However, exceptions have been reported in recent years,^{11–14,16,40} e.g., the $SDS@2\beta-CD$ system,^{13,16} the zwitterionic surfactant@ $\beta-CD$ hydrogel,¹¹ and the $C_{12}mimBr@\beta-CD$ system.⁴⁰ In the cationic surfactant solution, Jiang et al.⁵² and Wang et al.⁵³ suggested that $\beta-CD$

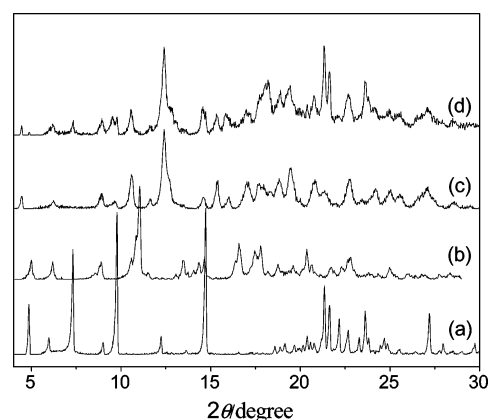


Figure 6. XRD patterns of (a) $C_{12}mimDSN$, (b) xerogel, (c) $\beta-CD$, and (d) physical mixture of $C_{12}mimDSN@3\beta-CD$.

would selectively bind the excess component of the cationic and anionic surfactant mixture but was not involved in forming the self-assemblies. However, in our work, the concentrations of $C_{12}mim^+$ and DSN^- are the same. We think that $\beta-CD$ contributes to dissolving the $C_{12}mimDSN$ precipitate and also takes part in forming the vesicle and the hydrogel. An excess amount of $\beta-CD$ was added into the $C_{12}mimDSN@3\beta-CD$ (4 mM@12 mM) solution, and the DLS results in Figure 2 show that the self-assemblies still exist, which strongly suggests that $\beta-CD$ does not destroy the vesicle. The increase of the vesicle size with the addition of $\beta-CD$ in Figure 2 should be attributed to the aggregates consisting of the excess $\beta-CD$ in the solution. This is observed by the TEM method in Figure 3G, where we can find the coexistence of the vesicle and the sheet-shaped $\beta-CD$ aggregate.^{15,62}

The building block of the self-assemblies should be discussed afterward. In the $SDS@2\beta-CD$ vesicle system and our $C_{12}mimBr@\beta-CD$ vesicle and supramolecular hydrogel system, the inorganic ion, i.e., Na^+ and Br^- , should be necessary to act as counterions to keep the electrical neutrality of the self-assemblies. However, in the $C_{12}mimDSN@3\beta-CD$ system, if the $C_{12}mim^+-\beta-CD$ and $DSN^--\beta-CD$ formed the vesicles, they would aggregate with each other via electrostatic interaction as there are no inorganic ions in the system. We think that the $C_{12}mim^+-\beta-CD$ and $DSN^--\beta-CD$ inclusion complexes tend to bind with each other to keep the electrical neutrality of the self-assembly. Therefore, we can conclude that the building block of the self-assemblies is formed by both $C_{12}mim^+-\beta-CD$ and $DSN^--\beta-CD$ inclusion complexes.

HRMS of the $C_{12}mimDSN@3\beta-CD$ (4 mM@12 mM) system was examined, and the results are shown in Figure 7. We can find signals corresponding to the 1:1 ($C_{12}mim + \beta-CD$)⁺ and ($DSN + \beta-CD$)⁻ complexes, and a signal corresponding to the 1:2 ($C_{12}mim + 2\beta-CD$)⁺ complex, but no signals corresponding to the 1:2 ($DSN + 2\beta-CD$)⁻ complex. According to our previous study about the multiple equilibria interaction pattern between imidazolium-based ILs and $\beta-CD$,^{38,39} $C_{12}mim^+$ can form both the 1:1 and 1:2 $\beta-CD$ inclusion complexes with large association constants. Competitive fluorescence measurement experiment was conducted to study the interaction between $SDSN$ and $\beta-CD$. The K_1' and K_2' value for 1/ $\beta-CD$ system are 1200 ± 220 and $2300 \pm 130 M^{-1}$, which are close to the results in our previous study.⁶³ The fitting curves of the 1:1 and 1:2 inclusion model is shown in Figure 8. The association constants K_1 and K_2 for the

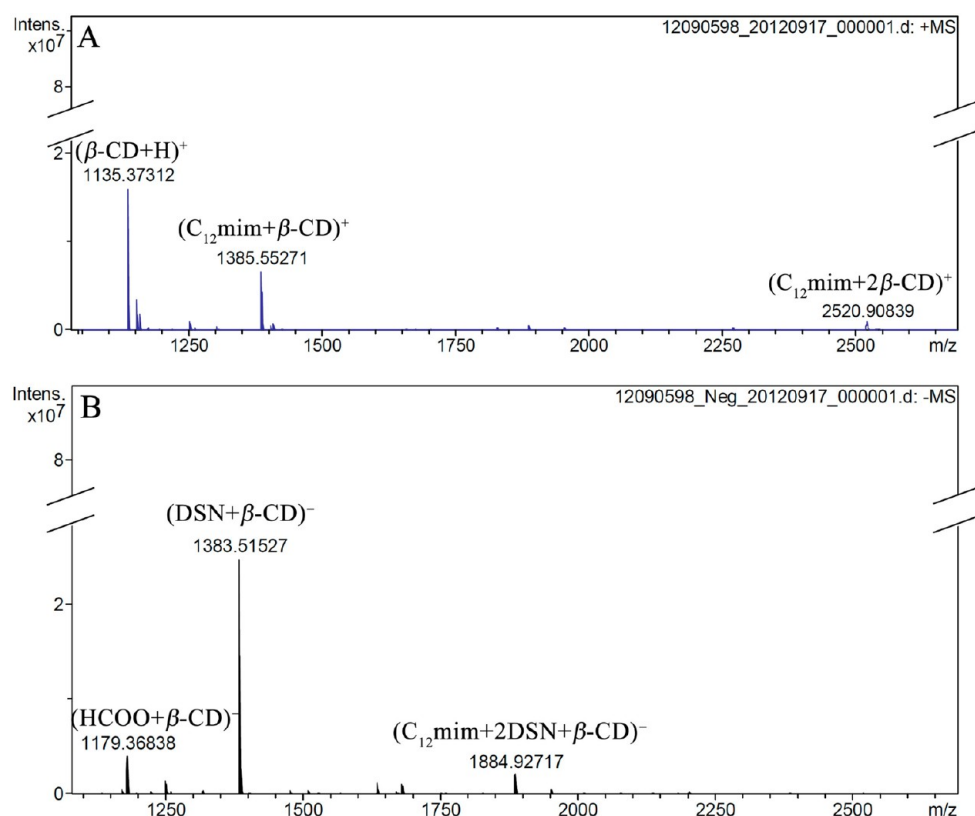


Figure 7. HRMS spectra of the $C_{12}mimDSN@3\beta-CD$ (4 mM@12 mM) solution: (A) positive spectrum and (B) negative spectrum.

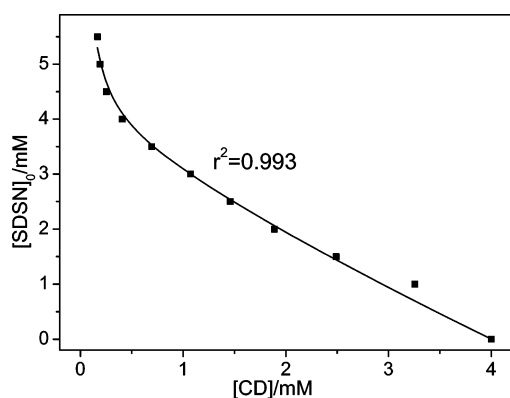


Figure 8. Initial concentration of SDSN vs the equilibrium concentration of $\beta-CD$. The solid line is the nonlinear regression fit to the experimental data points following the model of 1:1 and 1:2.

SDSN- $\beta-CD$ system are estimated to be $15\,300 \pm 1100$ and $32 \pm 22\ M^{-1}$. The K_2 value is quite small, indicating that there exists only a very minor amount, if any, of the 1:2 complexes, so no signals of the $(DSN + 2\beta-CD)^-$ complex can be detected in the HRMS spectrum.

Therefore, taking into consideration the HRMS spectra, the competitive fluorescence measurement results, and the 1:3 molar ratio of the $C_{12}mimDSN@3\beta-CD$ system, we may deduce that $C_{12}mim^+$ mainly forms the 1:1 and the 1:2 inclusion complexes, while DSN^- mainly forms the 1:1 inclusion complexes with $\beta-CD$ in the building block of the supramolecular self-assemblies. The $C_{12}mim^+ - 2\beta-CD$ inclusion complex interacts with the $DSN^- - \beta-CD$ complex to form the $C_{12}mimDSN@3\beta-CD$ system, and the remaining 1:1 $C_{12}mim^+ - \beta-CD$ complex interacts with either the $DSN^- - \beta-$

CD complex and the uncomplexed $\beta-CD$ or the minor amount of the $DSN^- - 2\beta-CD$ complex to form the building blocks. The above processes are illustrated in Scheme 3. In the $C_{12}mim^+ - 2\beta-CD$ inclusion complexes, two $\beta-CD$ molecules should be preferably aligned in a head-to-head structure to maximize the formation of H-bonds.^{13,64,65}

Then how do the inclusion complexes assemble into the building block? The most possible model is that they bind tail-to-tail with each other to form a more hydrophilic structure, which is common in the self-assembly structures of the cationic surfactant system.⁴⁷⁻⁴⁹ After comparing the length of the dodecyl chain (14.9 Å) with the height of three $\beta-CD$ s in stacks (23.7 Å), we think that the alkyl chains of $C_{12}mim^+$ and DSN^- may intersect to some extent with each other like the structure I in Scheme 3. In the $C_{12}mimBr@3\beta-CD$ system, the $^1H-^1H$ ROESY method was employed to study the spatial noncovalent interaction in the supramolecular systems, and the resonance correlations between 2-H and 4-H of $C_{12}mimBr$ revealed that the alkyl side chains of two $C_{12}mim^+$ have interaction with each other.⁴⁰ In this work, the resonance correlations marked with squares in Figure 9 suggest the interaction between 1-H and 2-H, which are the tail end of the alkyl side chains. There is no further intersection because there stack three CD molecules (23.7 Å) in the $C_{12}mimDSN@3\beta-CD$ building block, and the dodecyl chains of the $C_{12}mim^+$ and DSN^- are not long enough for further intersection.

On the basis of structure I, we have proposed the schematic self-assembly mechanism of the formation of the vesicle and the supramolecular hydrogel in Scheme 3. Because of the electrostatic interaction, two building blocks will probably form head-to-tail pairs, which can further grow into a lamellar structure. At low $C_{12}mimDSN@3\beta-CD$ concentration, the

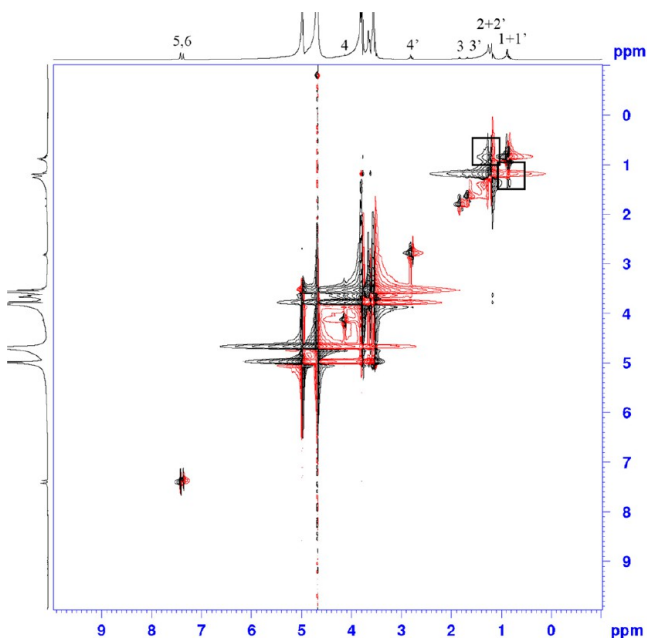
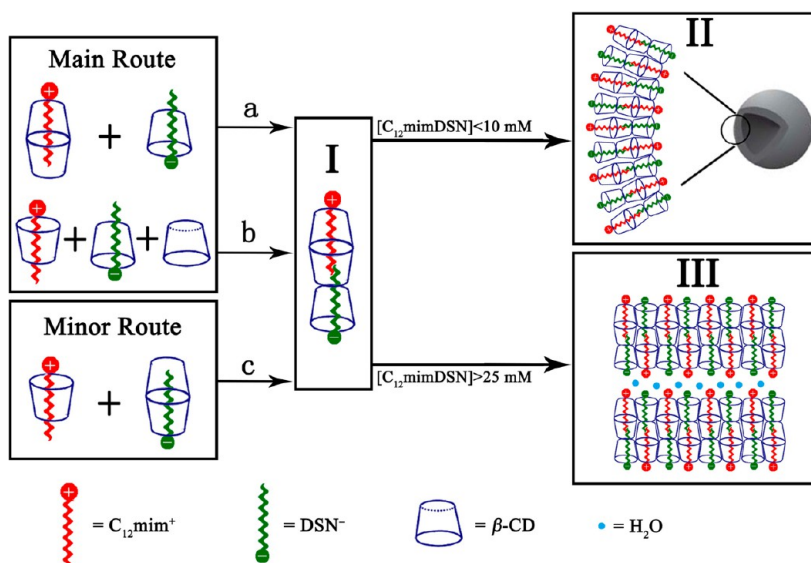
Scheme 3. Mechanism of the Formation of the Vesicle and the Supramolecular Hydrogel by the C_{12} mimDSN@ 3β -CD Complexes

Figure 9. ^1H - ^1H ROESY NMR spectrum of C_{12} mimDSN@ 3β -CD (4 mM@12 mM) solution in D_2O at 400 MHz and $T = 298$ K.

lamellar structure spontaneously forms the spherical vesicle (Scheme III). At the relative high concentration, the lamella stacks layer-by-layer into hydrogel (Scheme III). The binding force between hydrogel layers is believed to be the H-bonding network comprising the C_{12} mim $^+$, DSN $^-$, and water molecules involved in the gel framework. Around the medium concentration, the solution turns out to be turbid at room temperature. We think that the increase of concentration will probably lead to a vesicle-to-hydrogel transition.¹⁵ As shown in Figure 3H, microsize sheets together with vesicles are observed in the C_{12} mimDSN@ 3β -CD (15 mM@45 mM) solution. However, owing to the low concentration, the sheet structure does not form a hydrogel but a precipitate instead.

Driving Force of Self-Assembly. Electrostatic Interaction. In the self-assemblies, the electrostatic interaction may

play a prominent role in maintaining the structure of the vesicle and the hydrogel. To prove it, control experiments were conducted to disturb the electrostatic interaction¹⁶ by adding 16 mM NaBr into C_{12} mimDSN@ 3β -CD (4 mM@12 mM) vesicle system and 60 mM NaBr into C_{12} mimDSN@ 3β -CD (30 mM@90 mM) hydrogel system. It was found that the vesicle amount was markedly decreased when the solution was characterized by TEM method (see Figure S1 of the Supporting Information), and the hydrogel disassembled into a turbid emulsion because of the presence of NaBr (Scheme S1). The inorganic ions in the solution shield the electrostatic interaction between C_{12} mim $^+$ and DSN $^-$ and thus hinder the further self-assembly of the C_{12} mimDSN@ 3β -CD building block. Besides, the decrease of vesicle amount and the disassembly of hydrogel were also observed in the experiments that other salts, e.g., NaCl, MgCl_2 , and $\text{Al}(\text{NO}_3)_3$, were used instead of NaBr. When 16 mM MgCl_2 or $\text{Al}(\text{NO}_3)_3$ was added into the C_{12} mimDSN@ 3β -CD (4 mM@12 mM) system, the DLS results (Figure S2) show that only peaks around 1 nm exist. The DLS results were plotted with relative number as ordinate, so it turns out that β -CD inclusion complexes are the main aggregate and few vesicles exist.

Hydrophobic Interaction between Alkyl Chains and β -CD Cavity. Moreover, we discuss herein the characteristic of both C_{12} mimDSN and β -CD in the C_{12} mimDSN@ 3β -CD system by substituting them with similar molecules, and the results are listed in Table 1. In the corresponding C_n mimDSN@ 3β -CD systems, both vesicle and hydrogel were obtained in C_{12} mimDSN@ 3β -CD, C_{10} mimDSN@ 3β -CD, and C_8 mimDSN@ 3β -CD solutions, while in C_6 mimDSN@ 3β -CD solution, no self-assembly was found. The difference in the length of the C_n mim $^+$ alkyl chain should be the reason. The length of the C_6 mim $^+$ alkyl chain is too short to intersect with DSN $^-$; thus, no C_6 mimDSN@ 3β -CD building block can be formed. This reflects the significance of the hydrophobic interaction between the alkyl chains and the β -CD cavity to the self-assembly. Besides, other kinds of CDs were also employed instead of β -CD in the C_{12} mimDSN@ 3β -CD system. In the corresponding α -CD and γ -CD systems in Table 1, only precipitation takes place. Their improper cavity sizes may

Table 1. Formation of Vesicle and Hydrogel in Different Systems^a

	vesicle	hydrogel
C ₁₂ mimDSN@3β-CD	F	F
C ₁₀ mimDSN@3β-CD	F	F
C ₈ mimDSN@3β-CD	F	F
C ₆ mimDSN@3β-CD	N	N*
CTAB@β-CD ⁴⁰	F	N*
CTA-DSN@3β-CD	N*	N*
C ₁₂ mimDSN@3DM-β-CD	F	F
C ₁₂ mimDSN@3HP-β-CD	N*	N*
C ₁₂ mimDSN@3α-CD	N*	N*
C ₁₂ mimDSN@3γ-CD	N*	N*

^aThe formation of vesicle by the negative-staining TEM and FFTEM methods. The concentration of the BAIL@3CD solution for the study of vesicle is 5 mM; 15 mM, and that for the study of hydrogel is 40 mM; 120 mM. In CTAB@β-CD system, the concentrations are both 250 mM. F: formation; N: no formation. *Precipitation.

obstruct them from forming the intersection between the alkyl chains; thus, the C₁₂mimDSN@3CD building block cannot be formed.

H-Bonding between Neighboring β-CDs. We have discussed above that the intermolecular H-bonding between neighboring β-CDs as well as between β-CD and water contributes a lot to the formation of the supramolecular hydrogel. In addition, C₁₂mimDSN@3DM-β-CD system formed vesicle and hydrogel, while precipitation took place in C₁₂mimDSN@3HP-β-CD system. In the secondary assembly of β-CD nanotube, the H-bonding between the hydroxyl groups of neighboring CDs was believed to contribute to the formation of the nanotubular structure.^{61,66} In our C₁₂mimDSN@3CD system here, the H-bonding should also contribute to the stack of three CD molecules and the head-to-tail binding of two building blocks. HP-β-CD is a kind of "H-bond-poor" CD,¹⁶ and DM-β-CD can still form an H-bond. The result here suggests that the H-bonding of CD contributes to the formation of the self-assemblies.

Interaction between Imidazolium Headgroup and Water. In the CTAB@β-CD (250 mM@250 mM) solution, it was discovered that vesicle could be formed, whereas hydrogel could not.⁴⁰ Comparing it with the C₁₂mimBr@β-CD self-assembly system, we suggested that the imidazolium headgroup of C₁₂mimBr plays an important role in the formation of the hydrogel.⁴⁰ It has been found before that the aromatic C–H on the imidazolium group can easily form an H-bond with water molecules.^{67–69} Therefore, the H-bond network between the imidazolium headgroup and the water molecule involved in the hydrogel should contribute to forming the lamellar structure of the hydrogel. However, in the CTA-DSN@3β-CD system, only a white precipitate was obtained in either diluted or concentrated solutions. In the diluted solution, the solubility of CTA-DSN in the aqueous solution was measured to be less than 0.1 mM, and the binding ability of β-CD to the CTA⁺ and DSN[−] may be not strong enough to destroy the crystal lattice of the CTA-DSN to form the building block; thus the CTA-DSN precipitated. In the concentration system, compared with the C₁₂mimDSN@3β-CD hydrogel in this work, there lacks the H-bonding between the imidazolium headgroup of C₁₂mim⁺ and water, so no hydrogel can be formed. These results demonstrate that the H-bond interaction between the imidazolium headgroup and the water molecules in the

hydrogel is the driving force for self-assembly of the C₁₂mimDSN@3β-CD hydrogel.

CONCLUSIONS

On the basis of our previous study about C₁₂mimBr@β-CD supramolecular self-assembly system, we have synthesized a new kind of BAIL C₁₂mimDSN and systematically investigated the self-assembling behavior with β-CD in aqueous solution. The vesicle and the supramolecular hydrogel are obtained in the C₁₂mimDSN@3β-CD aqueous solution at different concentrations. The building block for the supramolecular self-assemblies is determined to be the C₁₂mimDSN@3β-CD complex, in which the alkyl chains of C₁₂mim⁺ and DSN[−] intersect with each other in the cavity of three β-CDs. We propose a novel self-assembly mechanism that the building block laterally binds head-to-tail with each other to form the lamellae structure, which is apparently different from that of the C₁₂mimBr@β-CD system.⁴⁰ These results strongly suggest that both the cation and anion of BAILS can self-assemble with β-CD in the aqueous solution. By extending this self-assembly to other BAIL@3CD systems, we find that the driving force for the self-assembly includes the electronic interaction between cation and anion of the C₁₂mimDSN, the hydrophobic interaction between the alkyl chains of BAIL and β-CD cavity, H-bonding between neighboring β-CDs, and the interaction between imidazolium headgroup and water in the hydrogel. This vesicle and supramolecular hydrogel system may be useful in the field of biomedical applications and act as a template for inorganic synthesis.

ASSOCIATED CONTENT

Supporting Information

Figures S1 and S2; Scheme S1. This material is available free of charge via the Internet at <http://pubs.acs.org>.

AUTHOR INFORMATION

Corresponding Author

*Tel 86-10-62765915; Fax 86-10-62759191; e-mail xshen@pku.edu.cn (X.S.).

Notes

The authors declare no competing financial interest.

ACKNOWLEDGMENTS

The authors are grateful to Mr. Jingxin Yang (Beijing NMR Center) for his help in ¹H–¹H ROESY NMR measurement. This work was financially supported by National Natural Science Foundation of China (Grant Nos. 91226112 and 20871009).

REFERENCES

- Wenz, G. Cyclodextrins as Building-Blocks for Supramolecular Structures and Functional Units. *Angew. Chem., Int. Ed.* **1994**, *33*, 803–822.
- Szejtli, J. Introduction and General Overview of Cyclodextrin Chemistry. *Chem. Rev.* **1998**, *98*, 1743–1753.
- Liu, Y.; Chen, Y. Cooperative Binding and Multiple Recognition by Bridged Bis(β-Cyclodextrin)s with Functional Linkers. *Acc. Chem. Res.* **2006**, *39*, 681–691.
- Song, L. X.; Bai, L.; Xu, X. M.; He, J.; Pan, S. Z. Inclusion Complexation, Encapsulation Interaction and Inclusion Number in Cyclodextrin Chemistry. *Coord. Chem. Rev.* **2009**, *253*, 1276–1284.
- Harada, A.; Takashima, Y.; Yamaguchi, H. Cyclodextrin-Based Supramolecular Polymers. *Chem. Soc. Rev.* **2009**, *38*, 875–882.

- (6) Astray, G.; Gonzalez-Barreiro, C.; Mejuto, J. C.; Rial-Otero, R.; Simal-Gandara, J. A Review on the Use of Cyclodextrins in Foods. *Food Hydrocolloids* **2009**, *23*, 1631–1640.
- (7) Del Valle, E. M. M. Cyclodextrins and Their Uses: A Review. *Process Biochem.* **2004**, *39*, 1033–1046.
- (8) Wang, J.; Jiang, M. Polymeric Self-Assembly into Micelles and Hollow Spheres with Multiscale Cavities Driven by Inclusion Complexation. *J. Am. Chem. Soc.* **2006**, *128*, 3703–3708.
- (9) Tao, W.; Liu, Y.; Jiang, B. B.; Yu, S. R.; Huang, W.; Zhou, Y. F.; Yan, D. Y. A Linear-Hyperbranched Supramolecular Amphiphile and Its Self-Assembly into Vesicles with Great Ductility. *J. Am. Chem. Soc.* **2012**, *134*, 762–764.
- (10) Sun, T.; Yan, H.; Liu, G. C.; Hao, J. C.; Su, J.; Li, S. Y.; Xing, P. Y.; Hao, A. Y. Strategy of Directly Employing Paclitaxel To Construct Vesicles. *J. Phys. Chem. B* **2012**, *116*, 14628–14636.
- (11) Jiang, L. X.; Yan, Y.; Huang, J. B. Zwitterionic Surfactant/Cyclodextrin Hydrogel: Microtubes and Multiple Responses. *Soft Matter* **2011**, *7*, 10417–10423.
- (12) Xu, H. N.; Ma, S. F.; Chen, W. Unique Role of β -Cyclodextrin in Modifying Aggregation of Triton X-114 in Aqueous Solutions. *Soft Matter* **2012**, *8*, 3856–3863.
- (13) Jiang, L. X.; Peng, Y.; Yan, Y.; Huang, J. B. Aqueous Self-Assembly of SDS@2 β -CD Complexes: Lamellae and Vesicles. *Soft Matter* **2011**, *7*, 1726–1731.
- (14) Jing, B.; Chen, X.; Wang, X. D.; Yang, C. J.; Xie, Y. Z.; Qiu, H. Y. Self-Assembly Vesicles Made From a Cyclodextrin Supramolecular Complex. *Chem.—Eur. J.* **2007**, *13*, 9137–9142.
- (15) Zhou, C. C.; Cheng, X. H.; Zhao, Q.; Yan, Y.; Wang, J. D.; Huang, J. B. Self-Assembly of Nonionic Surfactant Tween 20@2 β -CD Inclusion Complexes in Dilute Solution. *Langmuir* **2013**, *29*, 13175–13182.
- (16) Jiang, L. X.; Peng, Y.; Yan, Y.; Deng, M. L.; Wang, Y. L.; Huang, J. B. “Annular Ring” Microtubes Formed by SDS@2 β -CD Complexes in Aqueous Solution. *Soft Matter* **2010**, *6*, 1731–1736.
- (17) Park, C.; Lee, I. H.; Lee, S.; Song, Y.; Rhue, M.; Kim, C. Cyclodextrin-Covered Organic Nanotubes Derived from Self-Assembly of Dendrons and Their Supramolecular Transformation. *Proc. Natl. Acad. Sci. U. S. A.* **2006**, *103*, 1199–1203.
- (18) Ogoshi, T.; Takashima, Y.; Yamaguchi, H.; Harada, A. Chemically-Responsive Sol-Gel Transition of Supramolecular Single-Walled Carbon Nanotubes (SWNTs) Hydrogel Made by Hybrids of SWNTs and Cyclodextrins. *J. Am. Chem. Soc.* **2007**, *129*, 4878–4879.
- (19) Deng, W.; Yamaguchi, H.; Takashima, Y.; Harada, A. Construction of Chemical-Responsive Supramolecular Hydrogels from Guest-Modified Cyclodextrins. *Chem.—Asian J.* **2008**, *3*, 687–695.
- (20) Peng, K.; Tomatsu, I.; Kros, A. Light Controlled Protein Release From a Supramolecular Hydrogel. *Chem. Commun.* **2010**, *46*, 4094–4096.
- (21) Park, J. S.; Jeong, S.; Chang, D. W.; Kim, J. P.; Kim, K.; Park, E. K.; Song, K. W. Lithium-Induced Supramolecular Hydrogel. *Chem. Commun.* **2011**, *47*, 4736–4738.
- (22) Welton, T. Room-Temperature Ionic Liquids. Solvents for Synthesis and Catalysis. *Chem. Rev.* **1999**, *99*, 2071–2083.
- (23) Opallo, M.; Lesniewski, A. A Review on Electrodes Modified with Ionic Liquids. *J. Electroanal. Chem.* **2011**, *656*, 2–16.
- (24) Xu, C.; Yuan, L. Y.; Shen, X. H.; Zhai, M. L. Efficient Removal of Caesium Ions from Aqueous Solution Using a Calix Crown Ether in Ionic Liquids: Mechanism and Radiation Effect. *Dalton Trans.* **2010**, *39*, 3897–3902.
- (25) Zhang, J. J.; Shen, X. H.; Chen, Q. D. Separation Processes in the Presence of Cyclodextrins Using Molecular Imprinting Technology and Ionic Liquid Cooperating Approach. *Curr. Org. Chem.* **2011**, *15*, 74–85.
- (26) Gao, Y. A.; Zhao, X. Y.; Dong, B.; Zheng, L. Q.; Li, N.; Zhang, S. H. Inclusion Complexes of β -Cyclodextrin with Ionic Liquid Surfactants. *J. Phys. Chem. B* **2006**, *110*, 8576–8581.
- (27) Francois, Y.; Varenne, A.; Sirieix-Plenet, J.; Gareil, P. Determination of Aqueous Inclusion Complexation Constants and Stoichiometry of Alkyl(Methyl)-Methylimidazolium-Based Ionic Liquid Cations and Neutral Cyclodextrins by Affinity Capillary Electrophoresis. *J. Sep. Sci.* **2007**, *30*, 751–760.
- (28) Li, N.; Liu, J.; Zhao, X. Y.; Gao, Y. A.; Zheng, L. Q.; Zhang, J.; Yu, L. Complex Formation of Ionic Liquid Surfactant and β -Cyclodextrin. *Colloids Surf., A* **2007**, *292*, 196–201.
- (29) Gao, Y. A.; Li, Z. H.; Du, J. M.; Han, B. X.; Li, G. Z.; Hou, W. G.; Shen, D.; Zheng, L. Q.; Zhang, G. Y. Preparation and Characterization of Inclusion Complexes of β -Cyclodextrin with Ionic Liquid. *Chem.—Eur. J.* **2005**, *11*, 5875–5880.
- (30) Subramaniam, P.; Mohamad, S.; Alias, Y. Synthesis and Characterization of the Inclusion Complex of Dicationic Ionic Liquid and β -Cyclodextrin. *Int. J. Mol. Sci.* **2010**, *11*, 3675–3685.
- (31) Singh, T.; Kumar, A. Aggregation Behavior of Ionic Liquids in Aqueous Solutions: Effect of Alkyl Chain Length, Cations, and Anions. *J. Phys. Chem. B* **2007**, *111*, 7843–7851.
- (32) Rao, K. S.; Singh, T.; Trivedi, T. J.; Kumar, A. Aggregation Behavior of Amino Acid Ionic Liquid Surfactants in Aqueous Media. *J. Phys. Chem. B* **2011**, *115*, 13847–13853.
- (33) Liu, X. F.; Dong, L. L.; Fang, Y. Synthesis and Self-Aggregation of a Hydroxyl-Functionalized Imidazolium-Based Ionic Liquid Surfactant in Aqueous Solution. *J. Surfactants Deterg.* **2011**, *14*, 203–210.
- (34) Huang, R. T. W.; Peng, K. C.; Shih, H. N.; Lin, G. H.; Chang, T. F.; Hsu, S. J.; Hsu, T. S. T.; Lin, I. J. B. Antimicrobial Properties of Ethoxyether-Functionalized Imidazolium Salts. *Soft Matter* **2011**, *7*, 8392–8400.
- (35) Jiao, J. J.; Dong, B.; Zhang, H. N.; Zhao, Y. Y.; Wang, X. Q.; Wang, R.; Yu, L. Aggregation Behaviors of Dodecyl Sulfate-Based Anionic Surface Active Ionic Liquids in Water. *J. Phys. Chem. B* **2012**, *116*, 958–965.
- (36) He, Y. F.; Shen, X. H. Interaction between β -Cyclodextrin and Ionic Liquids in Aqueous Solutions Investigated by a Competitive Method Using a Substituted 3H-Indole Probe. *J. Photochem. Photobiol., A* **2008**, *197*, 253–259.
- (37) He, Y. F.; Chen, Q. D.; Xu, C.; Zhang, J. J.; Shen, X. H. Interaction between Ionic Liquids and β -Cyclodextrin: A Discussion of Association Pattern. *J. Phys. Chem. B* **2009**, *113*, 231–238.
- (38) Zhang, J. J.; Shen, X. H. Multiple Equilibria Interaction Pattern between the Ionic Liquids $C_n\text{mimPF}_6$ and β -Cyclodextrin in Aqueous Solutions. *J. Phys. Chem. B* **2011**, *115*, 11852–11861.
- (39) Zhang, J. J.; Shi, J. F.; Shen, X. H. Further Understanding of the Multiple Equilibria Interaction Pattern between Ionic Liquid and β -Cyclodextrin. *J. Incl. Phenom. Macrocycl. Chem.* **2013**, DOI: 10.1007/s10847-013-0354-6.
- (40) Zhang, J. J.; Shen, X. H. Temperature-Induced Reversible Transition between Vesicle and Supramolecular Hydrogel in the Aqueous Ionic Liquid- β -Cyclodextrin System. *J. Phys. Chem. B* **2013**, *117*, 1451–1457.
- (41) Rao, K. S.; Trivedi, T. J.; Kumar, A. Aqueous-Biampiphilic Ionic Liquid Systems: Self-Assembly and Synthesis of Gold Nanocrystals/Microplates. *J. Phys. Chem. B* **2012**, *116*, 14363–14374.
- (42) Wang, K.; Yin, H. Q.; Sha, W.; Huang, J. B.; Fu, H. L. Temperature-Sensitive Aqueous Surfactant Two-Phase System Formation in Cationic - Anionic Surfactant Systems. *J. Phys. Chem. B* **2007**, *111*, 12997–13005.
- (43) Marques, E. F.; Brito, R. O.; Silva, S. G.; Rodriguez-Borges, J. E.; do Vale, M. L.; Gomes, P.; Araujo, M. J.; Soderman, O. Spontaneous Vesicle Formation in Catanionic Mixtures of Amino Acid-Based Surfactants: Chain Length Symmetry Effects. *Langmuir* **2008**, *24*, 11009–11017.
- (44) Li, H. G.; Xin, X.; Kalwarczyk, T.; Kalwarczyk, E.; Niton, P.; Holyst, R.; Hao, J. C. Reverse Vesicles from a Salt-Free Catanionic Surfactant System: A Confocal Fluorescence Microscopy Study. *Langmuir* **2010**, *26*, 15210–15218.
- (45) Sun, W. J.; Shen, Y. W.; Hao, J. C. Phase Behavior and Rheological Properties of Salt-Free Catanionic TTAOH/DA/H₂O System in the Presence of Hydrophilic and Hydrophobic Salts. *Langmuir* **2011**, *27*, 1675–1682.

- (46) Silva, B. F. B.; Marques, E. F.; Olsson, U. Aqueous Phase Behavior of Salt-Free Catanionic Surfactants: the Influence of Solubility Mismatch on Spontaneous Curvature and Balance of Forces. *Soft Matter* **2011**, *7*, 225–236.
- (47) Song, S. S.; Zheng, Q. S.; Song, A. X.; Hao, J. C. Self-Assembled Aggregates Originated from the Balance of Hydrogen-Bonding, Electrostatic, and Hydrophobic Interactions. *Langmuir* **2012**, *28*, 219–226.
- (48) Long, P. F.; Hao, J. C. A Gel State from Densely Packed Multilamellar Vesicles in the Crystalline State. *Soft Matter* **2010**, *6*, 4350–4356.
- (49) Zhao, M. W.; Yuan, J.; Zheng, L. Q. Spontaneous Formation of Vesicles by N-Dodecyl-N-Methylpyrrolidinium Bromide (C_{12} MPB) Ionic Liquid and Sodium Dodecyl Sulfate (SDS) in Aqueous Solution. *Colloids Surf., A* **2012**, *407*, 116–120.
- (50) Yan, P.; Tang, J. N.; Xiao, J. X. Interaction between β -Cyclodextrin and Mixed Cationic-Anionic Surfactants (1): Thermodynamic Study. *J. Dispersion Sci. Technol.* **2007**, *28*, 617–621.
- (51) Yan, P.; Tang, J. N.; Xiao, J. X. Interaction between β -Cyclodextrin and Mixed Cationic-Anionic Surfactants (2): Aggregation Behavior. *J. Dispersion Sci. Technol.* **2007**, *28*, 623–626.
- (52) Jiang, L. X.; Deng, M. L.; Wang, Y. L.; Liang, D. H.; Yan, Y.; Huang, J. B. Special Effect of β -Cyclodextrin on the Aggregation Behavior of Mixed Cationic/Anionic Surfactant Systems. *J. Phys. Chem. B* **2009**, *113*, 7498–7504.
- (53) Wang, D.; Long, P. F.; Dong, R. H.; Hao, J. C. Self-Assembly in the Mixtures of Surfactant and Dye Molecule Controlled via Temperature and β -Cyclodextrin Recognition. *Langmuir* **2012**, *28*, 14155–14163.
- (54) Popowycz, A. M.S. Thesis, University of Montreal, 1991.
- (55) Skrabal, P.; Steiger, J.; Zollinger, H. Planarization of Benzylideneaniline. *Helv. Chim. Acta* **1975**, *58*, 800–814.
- (56) Shen, X. H.; Belletete, M.; Durocher, G. Studies of the Inclusion Complexation between a 3H-Indole and β -Cyclodextrin in the Presence of Urea, Sodium Dodecyl Sulfate, and 1-Propanol. *Langmuir* **1997**, *13*, 5830–5836.
- (57) Kondo, Y.; Uchiyama, H.; Yoshino, N.; Nishiyama, K.; Abe, M. Spontaneous Vesicle Formation from Aqueous-Solutions of Didodecylmethylammonium Bromide and Sodium Dodecyl Sulfate Mixtures. *Langmuir* **1995**, *11*, 2380–2384.
- (58) Tondre, C.; Caillet, C. Properties of the Amphiphilic Films in Mixed Cationic/Anionic Vesicles: A Comprehensive View from a Literature Analysis. *Adv. Colloid Interface Sci.* **2001**, *93*, 115–134.
- (59) Marechal, Y. The Molecular Structure of Liquid Water Delivered by Absorption Spectroscopy in the Whole IR Region Completed with Thermodynamics Data. *J. Mol. Struct.* **2011**, *1004*, 146–155.
- (60) Zhang, Y. M.; Deng, X. R.; Wang, L. C.; Wei, T. B. Inclusion Compounds Formation of Poly(Azomethine Ether)s and β -Cyclodextrin. *J. Macromol. Sci., Part A: Pure Appl. Chem.* **2008**, *45*, 289–294.
- (61) He, Y. F.; Shen, X. H.; Chen, Q. D.; Gao, H. C. Characterization and Mechanism Study of Micrometer-Sized Secondary Assembly of β -Cyclodextrin. *Phys. Chem. Chem. Phys.* **2011**, *13*, 447–452.
- (62) Bonini, M.; Rossi, S.; Karlsson, G.; Almgren, M.; Lo Nostro, P.; Baglioni, P. Self-Assembly of β -Cyclodextrin in Water. Part 1: Cryo-TEM and Dynamic and Static Light Scattering. *Langmuir* **2006**, *22*, 1478–1484.
- (63) Shen, X. H.; Belletete, M.; Durocher, G. Quantitative Study of the Hydrophobic Interaction Mechanism between Urea and Molecular Probes Used in Sensing Some Microheterogeneous Media. *J. Phys. Chem. B* **1997**, *101*, 8212–8220.
- (64) Funasaki, N.; Ishikawa, S.; Neya, S. 1:1 and 1:2 Complexes between Long-Chain Surfactant and α -Cyclodextrin Studied by NMR. *J. Phys. Chem. B* **2004**, *108*, 9593–9598.
- (65) Funasaki, N.; Ishikawa, S.; Hirota, S. Chemical Shifts as a Novel Measure of Interactions Between Two Binding Sites of Symmetric Dialkylmethylammonium Bromides to α -Cyclodextrin. *Anal. Chim. Acta* **2006**, *555*, 278–285.
- (66) Wu, A. H.; Shen, X. H.; He, Y. K. Micrometer-Sized Rodlike Structure Formed by the Secondary Assembly of Cyclodextrin Nanotube. *J. Colloid Interface Sci.* **2006**, *302*, 87–94.
- (67) Thar, J.; Brehm, M.; Seitsonen, A. P.; Kirchner, B. Unexpected Hydrogen Bond Dynamics in Imidazolium-Based Ionic Liquids. *J. Phys. Chem. B* **2009**, *113*, 15129–15132.
- (68) Mele, A.; Tran, C. D.; Lacerda, S. H. D. The Structure of a Room-Temperature Ionic Liquid with and without Trace Amounts of Water: The Role of C-H \cdots O and C-H \cdots F Interactions in 1-n-Butyl-3-Methylimidazolium Tetrafluoroborate. *Angew. Chem., Int. Ed.* **2003**, *42*, 4364–4366.
- (69) Zhang, Q. G.; Wang, N. N.; Yu, Z. W. The Hydrogen Bonding Interactions between the Ionic Liquid 1-Ethyl-3-Methylimidazolium Ethyl Sulfate and Water. *J. Phys. Chem. B* **2010**, *114*, 4747–4754.